Electronic Supplementary Material (ESI) for New Journal of Chemistry

CNTs synthesized with polyoxometalate-based metal-organic compounds as catalyst precursors *via* the CVD method and their adsorption performance for organic dyes

Yuan Tian, Xiu-Li Wang,* Jian Luan,* Hong-Yan Lin, Zhi-Han Chang, Xiang Wang, and Guo-Cheng Liu

X-Ray crystallography

Crystallographic data for compounds **1**−**4** were collected on a Bruker SMART APEX II with Mo Kα (λ =0.71073 Å) by ω and θ scan mode. All structures were solved by direct methods and refined on F^2 by full-matrix least squares using the SHELXL package (Sheldrick G. M.SHELXS-2014; University of Göttingen: Germany, 2014).[1] The command "DFIX" was used to refine atoms N10' N9' and N11' in compound **1**, O2 O6 O15 and O21 in **3**, C9 C10 C10 C12 C9' and C10' in **4**, the command "SIMU" was used to refine atoms C6 N8 N9 N10 N11 C6' N8' N9' N10' and N11' in compound **1**, AG1 and AG1' in compound **2**, the command "IOSR" was used to refine atoms O6 O15 O2 and O21 in compound **3**, C7 C13 C14 C19 C20 C7' C13' C14' C19' C20' C9 C10 C12 C9' and C10' in compound **4**, the command "EADP" was used to refine atoms O1W O1W' in compound **2**. All detailed crystal data and structures refinement for **1**−**4** were given in Table S1. For the compound **4**, there are strong van der Waals forces between the O7 atoms from PMo_{12}, and the distance is reasonable for donor and acceptor atoms. Crystallographic data for the structures reported in this paper have been deposited in the Cambridge Crystallographic Data Center with CCDC Numbers 1914987−1914990. Centre *via* www.ccdc.cam.ac.uk/data_request/cif.

Materials and measurements

The ligands 4-bptzp, 3-bptzp and 3-bptzpe were prepared according to a literature method [14]. All other chemicals were of commercial origin and used directly without further purification. The FT-IR spectra were performed on a Varian 640-IR spectrometer (KBr pellets). The elemental analyses (C, H and N) were carried out on a PerkinElmer 240C elemental analyzer. Powder X-ray diffraction (PXRD) patterns of powdered samples were performed using an Ultima IV with D/teX Ultra diffractometer at 40 kV, 40 mA with Cu Kα radiation. The morphology and structure of the CNT samples were characterized by scanning electron microscopy (SEM, Nova NanoSEM 430) and high resolution transmission electron microscopy (HRTEM, JEOL2010 at 200 kV). Laser Raman spectroscopy was used to estimate the quality of

the CNTs. The specific surface area and pore structure of the samples were investigated with an automatic volumetric sorption analyzer (ASAP 2020 M) using N_2 as the adsorbent at −196 °C. The UV−*vis* absorption spectra were obtained using a SP-1901 UV−*vis* spectrophotometer. The thermal stabilities of the CNTs were analyzed with a thermogravimetric analyzer (NETZSCH STA 449C). X-ray photoelectron spectroscopy (XPS) analyses were carried out with a Thermo SCIENTIFIC ESCALAB 250. Crystallographic data for compounds **1**−**4** were collected on a Bruker SMART APEX II with Mo Kα (λ =0.71073 Å) by ω and θ scan mode. The solution and refinement of crystal structures were listed in ESI. Crystallographic data for compounds **1**−**4** were shown in Table S2.

Preparation of compounds 1−4

Synthesis of {(4-H_2bptzb)$_2$[$HPMo_{12}O_{40}$]$_2$}·H_2O (1) A mixture of $AgNO_3$ (0.08 g, 0.47 mmol), 4-bptzp (0.015 g, 0.05 mmol), and $H_3[PMo_{12}O_{40}]$ (0.1 g, 0.05 mmol) was stirred in 20 ml deionized water and the pH value was adjusted to about 1.05 by 1 M HNO_3/$NH_3·H_2O$ solution. The suspension was transferred to a Teflon-lined autoclave (25 mL) and kept at 160 °C for 4 days. After slow cooling to room temperature, green block crystals of **1** were obtained. Yield 49.54% based on Mo. IR (KBr pellet, cm^{-1}): 3468(w), 2362(m), 1654(m), 1610(w), 1560(w), 1438(w), 1197(w), 1062(s), 958(s), 802(s), 694(m).

Synthesis of {Ag(4-H_2bptzb)(H_2O)[$PMo_{12}O_{40}$]}·H_2O (2) Compound **2** was obtained employing a similar procedure to that for **1**, except that the pH value was adjusted to about 1.00. Yellow block crystals of **2** were obtained. Yield 49.89% based on Mo. IR (KBr pellet, cm^{-1}): 2345(w), 1622(w), 1489(w), 1438(m), 1340(w), 1220(w), 1041(s), 935(s), 779(s).

Synthesis of {Ag_3(3-bptzb)$_2$[$PMo_{12}O_{40}$]} (3) Compound **3** was obtained with a similar procedure to that for **1**, except that 4-bptzp (0.015 g, 0.05 mmol) was replaced by 3-bptzp (0.015 g, 0.05 mmol) and the pH value was adjusted to about 1.97. Yellow block crystals of **3** were obtained. Yield 40.91% based on Mo. IR (KBr pellet, cm^{-1}): 2368(w), 1436(m), 1207(w), 1062(s), 958(s), 806(s), 694(m).

Synthesis of {Ag_4(3-bptzpe)$_3$(H_2O)$_2$[$HPMo_{12}O_{40}$]$_2$} (4) Compound **4** was obtained

similarly to **1**, except that 4-bptzb (0.015 g, 0.05 mmol) was replaced by 3-bptzpe (0.015 g, 0.05 mmol) and the pH value was adjusted to about 1.57. Yellow block crystals of **4** were obtained. Yield 50.18% based on Mo. IR (KBr pellet, cm^{-1}): 2368(w), 1654(m), 1062(s), 956(s), 875(s), 798(s).

Thermal stability analysis

As shown in Fig. S6, compounds **1**, **2** and **4** show two weight loss steps. The first weight loss step before 250 ℃ can be ascribed to the loss of the water molecules, 0.34% (calcd 0.38%) for **1**, 0.71% (calcd 0.78%) for **2**, 0.74%(calcd 0.69%) for **4**. The second weight loss step can be attributed to the decomposition of organic ligands and polyoxometalates, 25.85% (calc. 25.96%) for **1**, 17.86% (calc. 18.25%) for **2**, and 23.75% (calc. 23.52%) for **4**. While compound **3** shows only one weight loss step, which can be attributed to the decomposition of organic ligands and polyoxometalates 26.10% (calc. 26.16%) for **3**.

Preparation of the CNT 1-4

The above synthesized POM-based MOCs (100 mg) powder were placed in a quartz boat inside a quartz tube (diameter 80 mm, length 1100 mm) located in a horizontal electrical furnace. The furnace temperature was increased to 650 °C under an argon flow (300 mL min^{-1}, 99.999% purity) and kept for 65 min, then the catalyst precursor was reduced under a hydrogen atmosphere (200 mL min^{-1}, 99.999% purity) for 120 min. The synthesis of CNTs were performed at presence of the reduction of product under a gas mixture of C_2H_4 (25 mL min^{-1}), Ar (300 mL min^{-1}), and H_2 (200 mL min^{-1}) at 650 °C for 60 min. Then the system was cooled to room temperature under Ar flow, CNT 1-4 were thus synthesized by this procedure with compounds **1**−**4** as catalyst precursor, respectively.

Dye adsorption of the as prepared CNTs

In a typical experiment, the CNT powders (~5 mg) were put into the dye aqueous solution (9.2 mg L^{-1} for MB, 34 mg L^{-1} for MO and 8.4 mg L^{-1} for ST), followed by stirring at room temperature, respectively. Sample test were performed every 20 minutes by using a UV-vis spectrophotometer at the maximum absorbance of each dye (664 nm for MB, 465 nm for MO and 552 nm for ST). The dye adsorption

amount q_t (mg g^{-1}) was calculated by $q_t = (C_0 - C_t)V/W$, where C_0 and C_t (mg L^{-1}) were the liquid-phase concentrations of the dyes at the beginning and after time t (min), respectively. V (L) was the volume of the solution, and W (g) was the mass of CNT powder used .

Table S1 The coordination modes of N-donor ligands in compounds **2–4**

Compound	coordination modes of N-donor ligands
2	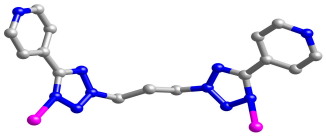
3	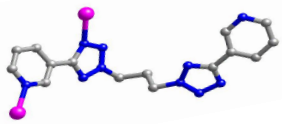
4	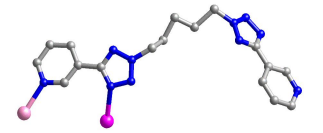 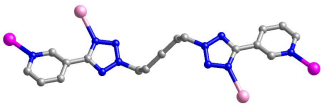

Table S2 Crystallographic data for compounds **1**−**4**

Compound	**1**	**2**	**3**	**4**
Empirical formula	$C_{45}H_{52}Mo_{24}N_{30}O_{82}P_2$	$C_{15}H_{20}AgMo_{12}N_{10}O_{42}P$	$C_{30}H_{28}Ag_3Mo_{12}N_{20}O_{40}P$	$C_{51}H_{60}Ag_4Mo_{24}N_{30}O_{82}P_2$
Formula weight	4689.66	2302.53	2814.58	5201.27
Crystal system	Triclinic	Monoclinic	Triclinic	Triclinic

Space group	*P-1*	*P2(1)/c*	*P-1*	*P-1*
a (Å)	13.2175(5)	13.0834(6)	10.7949(5)	13.2392(9)
b (Å)	13.7136(5)	13.2670(6)	12.2875(6)	13.5007(9)
c (Å)	16.3280(6)	27.2938(12)	13.5197(6)	16.4862(11)
α (°)	77.3500(10)	90	75.9810(10)	92.217(2)
β (°)	75.9590(10)	90.0270(10)	67.8830(10)	91.518(2)
γ (°)	77.6590(10)	90	75.6580(10)	100.322(2)
V (Å ^{3})	2760.87(18)	4737.6(4)	1587.23(13)	2895.2(3)
Z	1	4	1	1
D_c (g cm^{-3})	2.818	3.232	2.945	2.976
μ (mm^{-1})	2.775	3.624	3.323	3.307
F (000)	2222	4348	1328	2446
Reflection collected	20290	34554	11934	18738
Unique reflections	13593	11786	7956	11883
parameters	824	737	499	887
R_{int}	0.0176	0.0309	0.017	0.0534
GOF	1.079	1.019	1.025	0.961
$R_1{}^a$ [$I > 2\sigma(I)$]	0.0346	0.0335	0.0442	0.0566
$wR_2{}^b$ (all data)	0.0996	0.0771	0.0991	0.1403

[a] $R_1 = \Sigma||F_o|-|F_c||/\Sigma|F_o|$, [b] $wR_2 = \Sigma[w(F_o^2-F_c^2)^2]/\Sigma[w(F_o^2)^2]^{1/2}$

Table S3 The dye adsorption amount of CNTs to MB, ST and MO in dark.

	MB	ST	MO
CNT-1	104.44 mg·g^{-1}	67.87 mg·g^{-1}	0 mg·g^{-1}
CNT-2	75.42 mg·g^{-1}	64.85 mg·g^{-1}	0 mg·g^{-1}
CNT-3	26.46 mg·g^{-1}	50.91 mg·g^{-1}	0mg·g^{-1}
CNT-4	105.69 mg·g^{-1}	68.31 mg·g^{-1}	205.32 mg·g^{-1}
CNT-4 Recycle	78.01 mg·g^{-1}	43.57 mg·g^{-1}	170.57 mg·g^{-1}

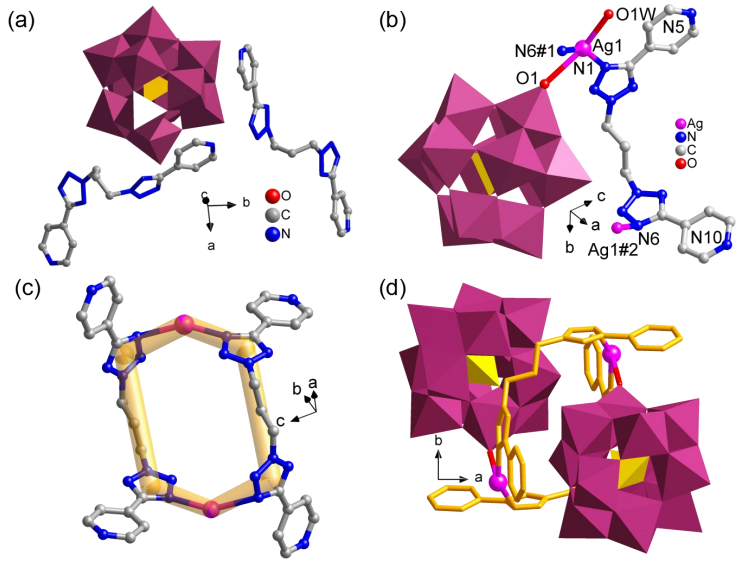

Fig. S1 (a) The structure of compound **1**; (b) The coordination environment of the Ag(I) ion in **2**, #1:-x,-y+2,-z; (c) The $[Ag_2(4\text{-}H_2bptzb)_2]^{6+}$ loop in **2**; (d) The discrete dinuclear structure of compound **2**.

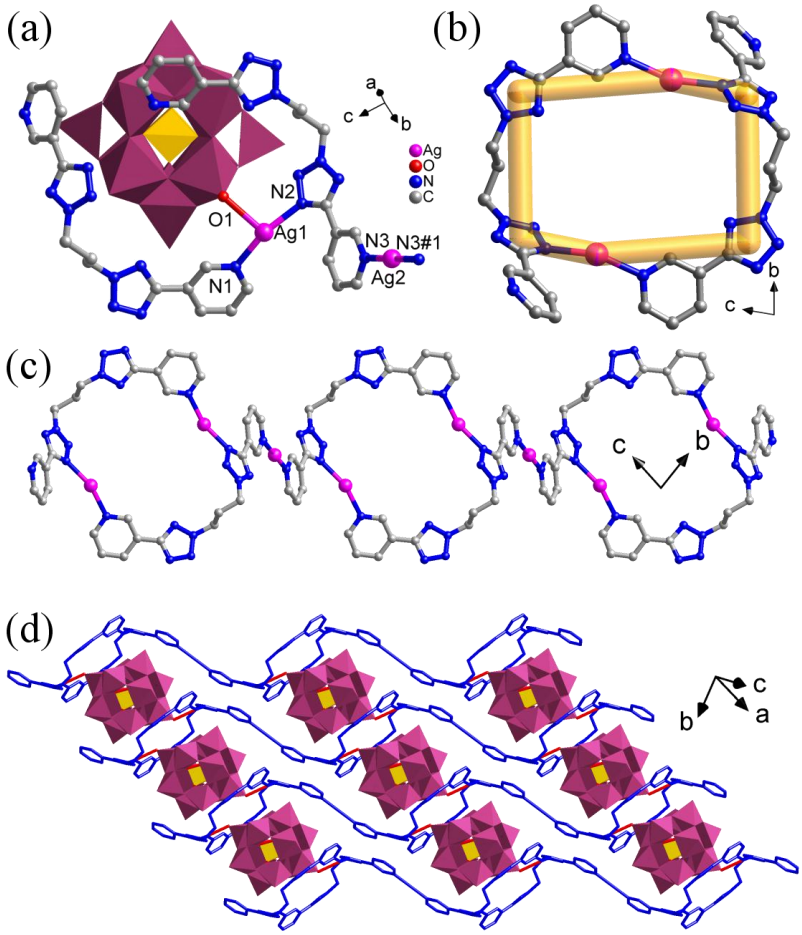

Fig. S2 (a) The coordination environment of the Ag(I) ions in **3**, #1:-x,-y+2,-z; (b)

The $[Ag_2(4\text{-bptzb})_2]^{2+}$ loop in **3**; (d) The 1D metal-organic chain in **3**; (d) The 2D layer in **3**.

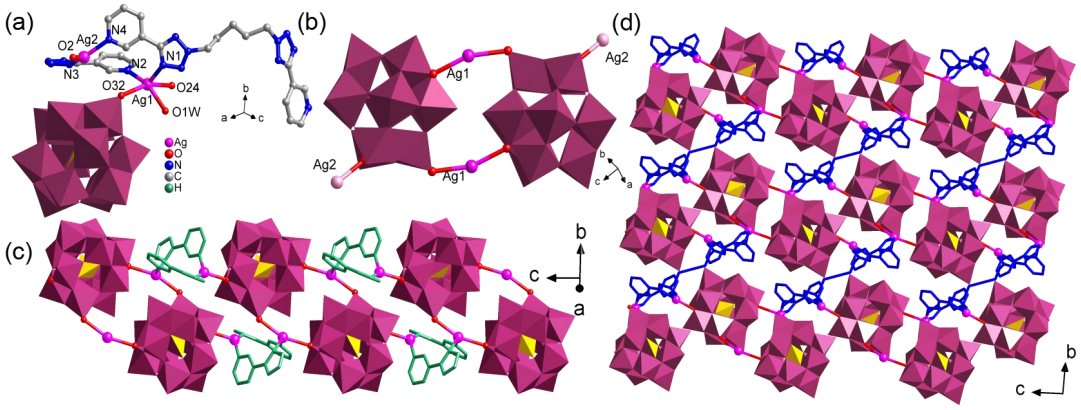

Fig.S 3 (a) The coordination environment of the Ag1 ion in **4**; (b) The $[Ag_4(PMo_{12})_2]$ metal-inorganic loop in **4**; (c) The 1D chain constructed from $[Ag_2(PMo_{12})_2]$ loops and 3-bptzpe ligands in **4**; (d) View of the 2D layer in **4**;

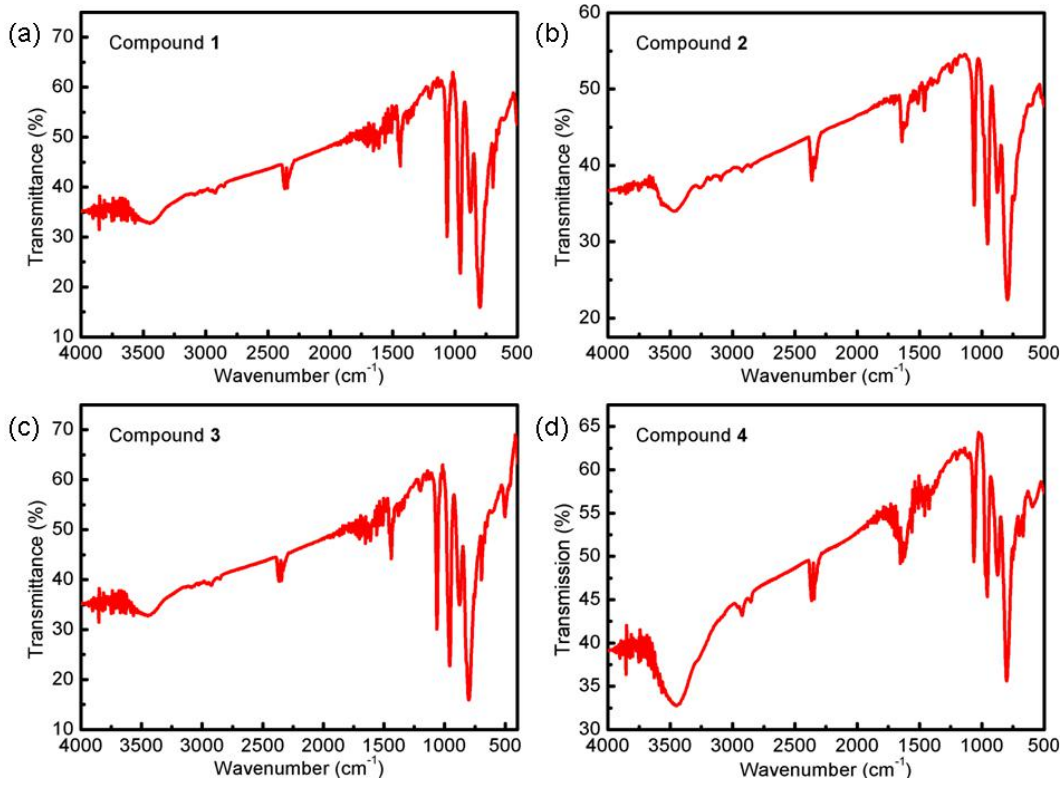

Fig. S4 The IR spectra of compounds **1**–**4**.

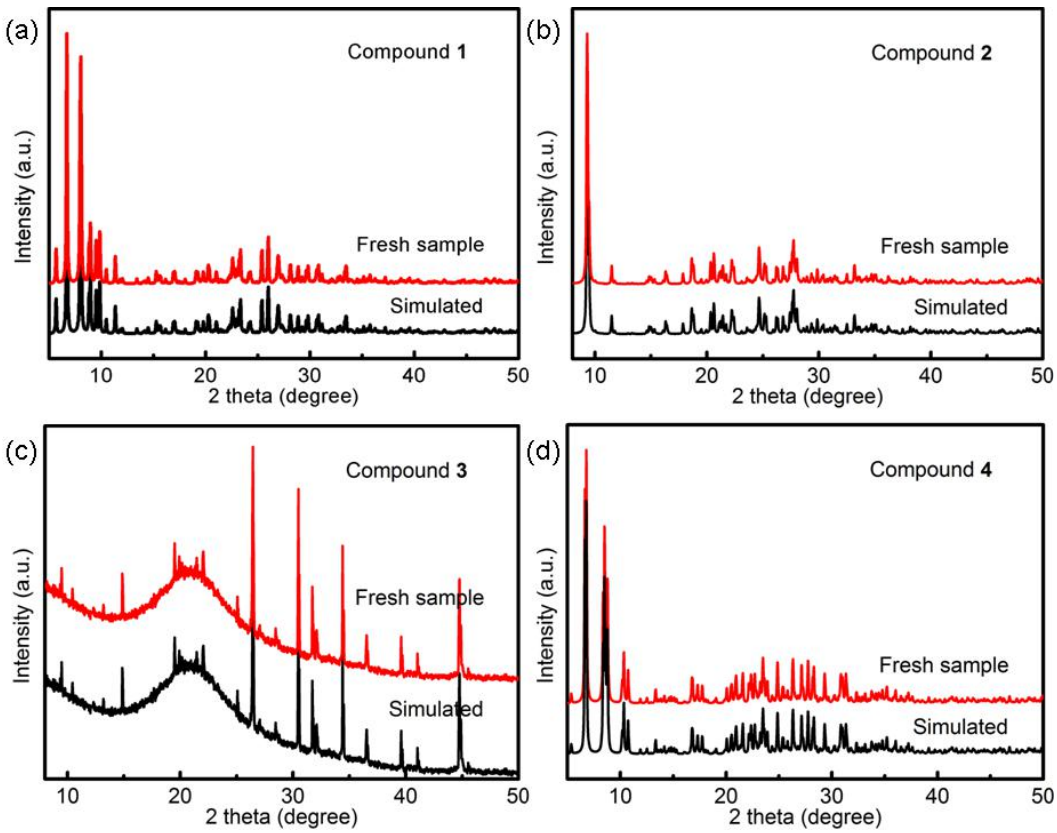

Fig. S5 PXRD patterns of compounds **1**–**4**.

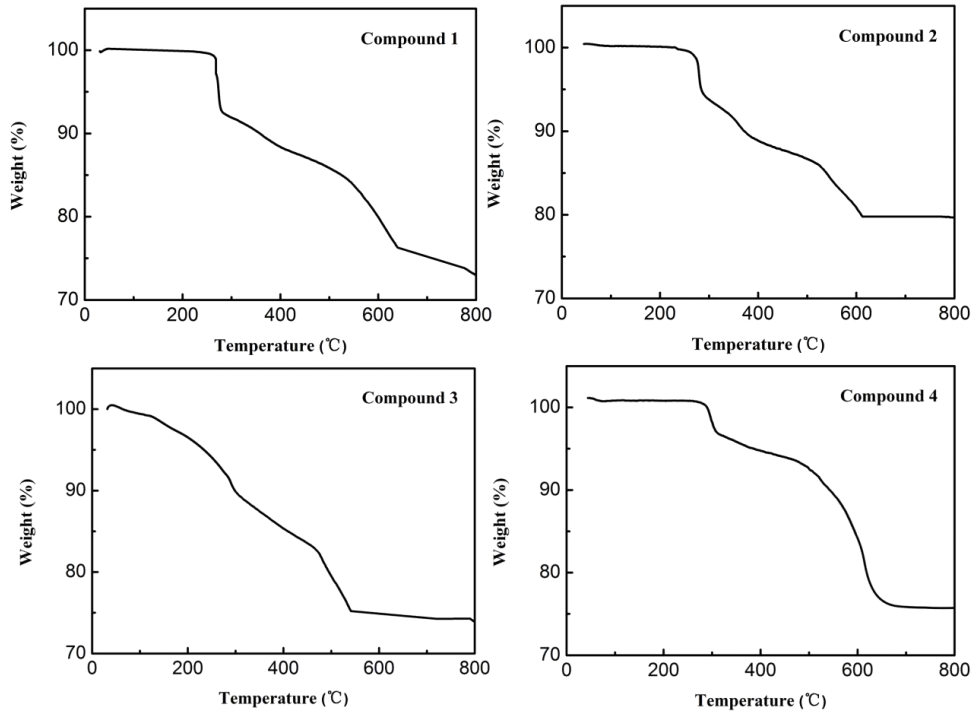

Fig. S6 TGA curves of compounds **1**–**4**.

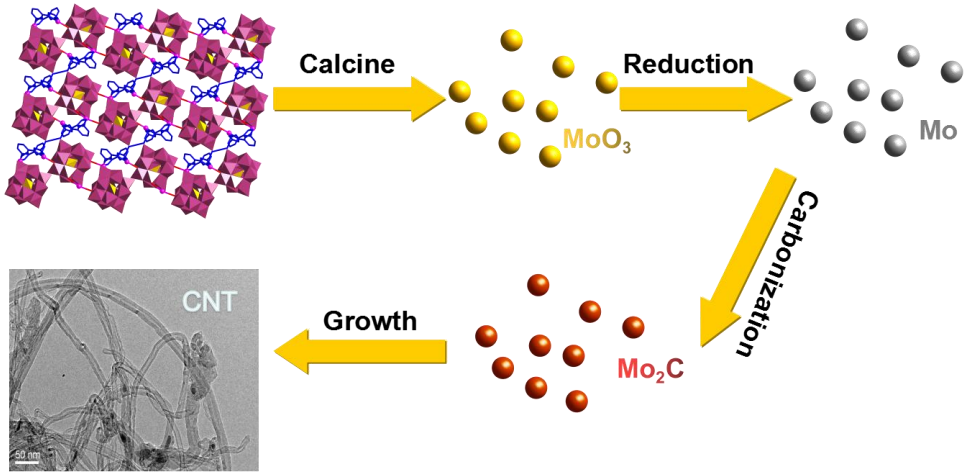

Fig. S7 The formation nanoparticles and the growth of CNTs.

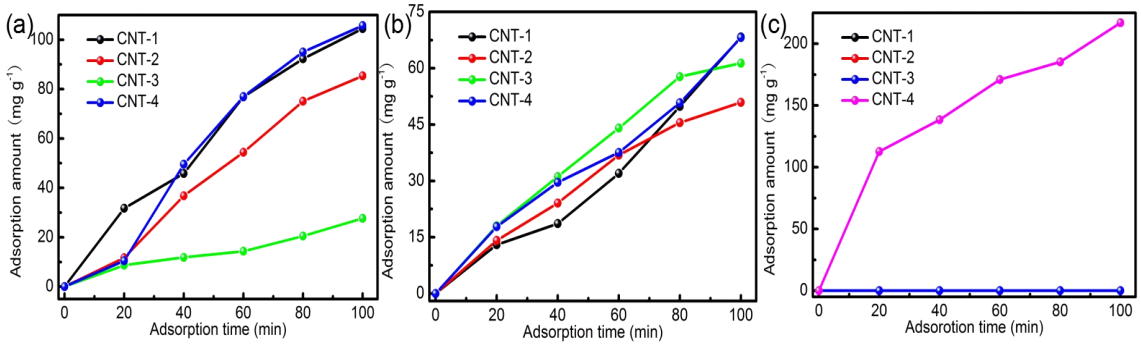

Fig. S8. The adsorption amount of MB (a), ST (b) and MO (c) within 100 min with CNT **1**–**4**.

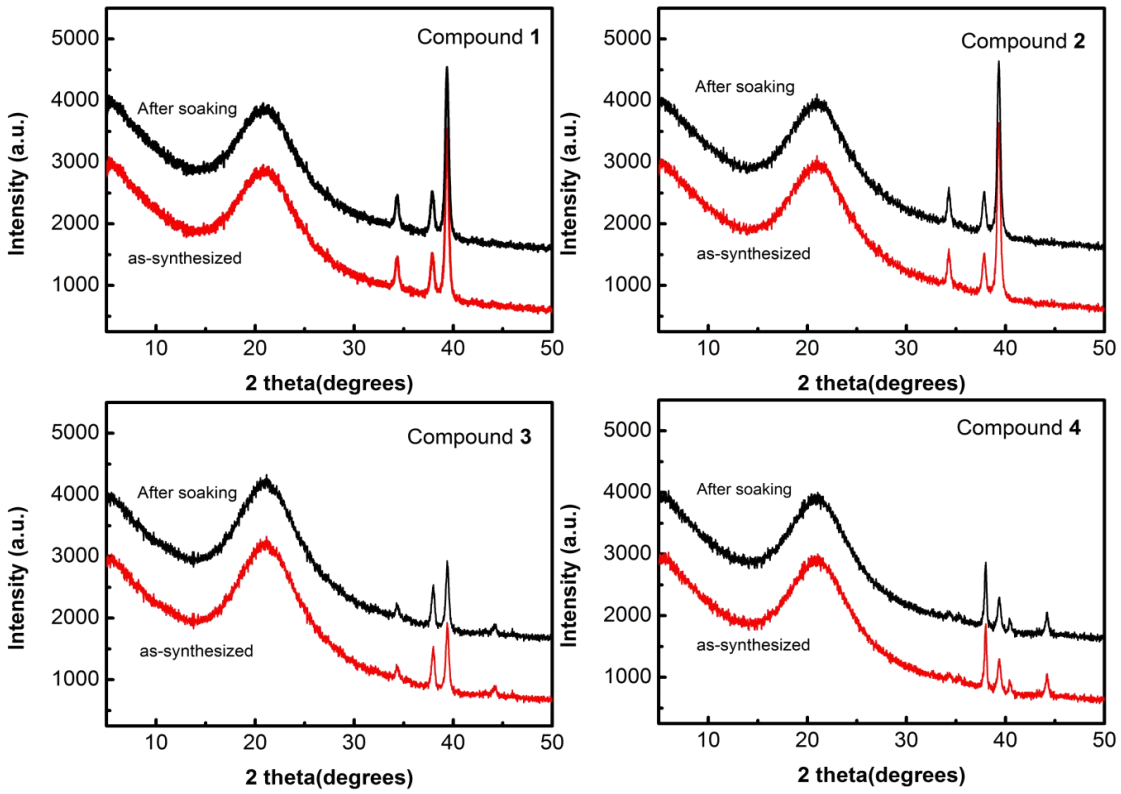

Fig. S9 PXRD patterns of CNTs in solutions and after drying in air.

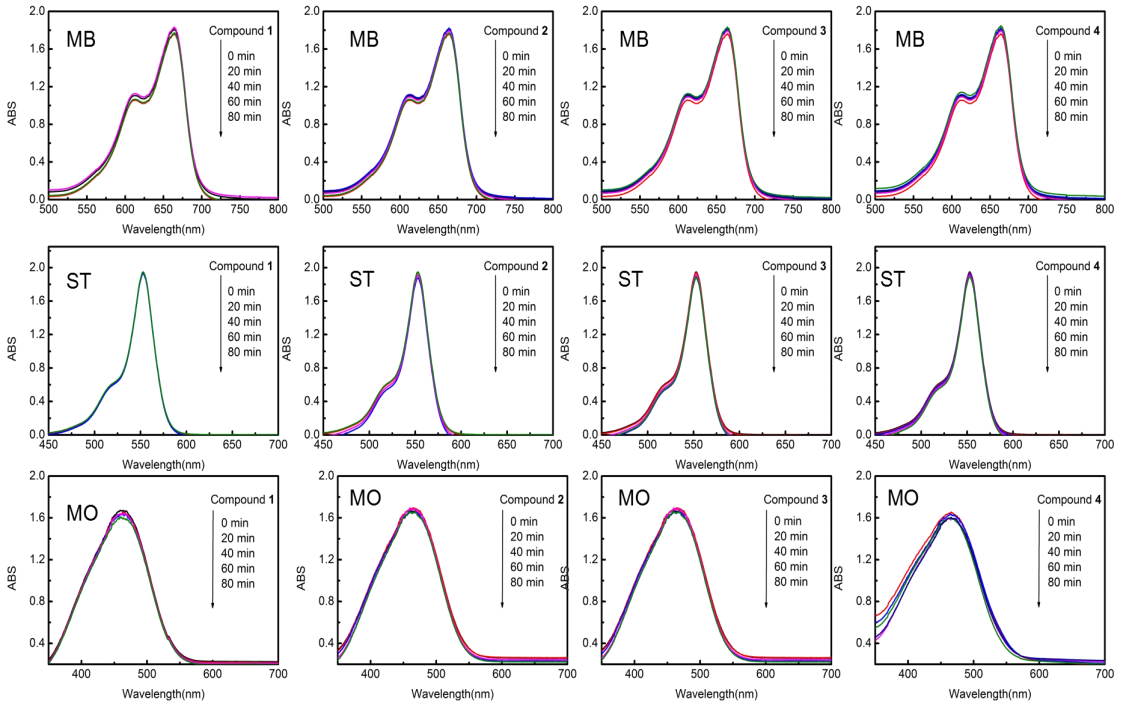

Fig. S10 Adsorption properties of compounds **1-4** for MB, ST and MO under dark conditions.

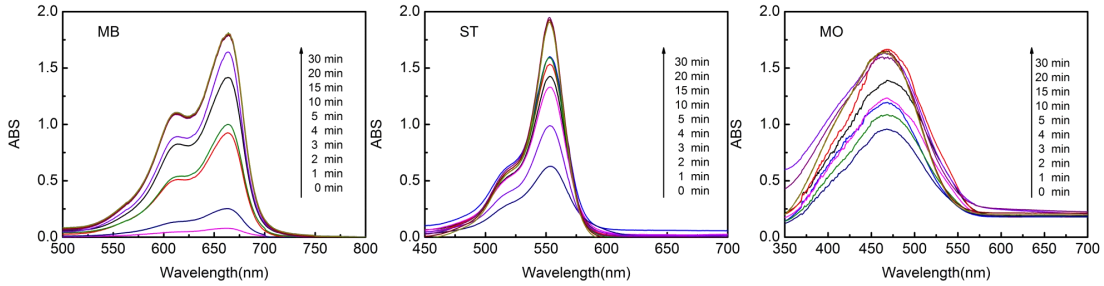

Fig. S11 The desorption properties of the CNT-**4** for MB/ST/MO.

References

1 G. M. Sheldrick, University of Göttingen, Germany Göttingen, **1997**.